HHS Public Access

Author manuscript

J Neurosci Methods. Author manuscript; available in PMC 2016 April 15.

Published in final edited form as:

J Neurosci Methods. 2015 April 15; 244: 104–113. doi:10.1016/j.jneumeth.2014.05.029.

Prefrontal cortical recordings with biomorphic MEAs reveal complex columnar-laminar microcircuits for BCI/BMI implementation

Ioan Opris[1,*], **Joshua L Fuqua**[1], **Greg A. Gerhardt**[2], **Robert E. Hampson**[1], and **Sam A. Deadwyler**[1,*]

[1]Department of Physiology and Pharmacology, Wake Forest University School of Medicine, Winston-Salem, North Carolina USA

[2]Department of Anatomy and Neurobiology, University of Kentucky, Lexington, KY, USA

Abstract

The mammalian prefrontal cortex known as the seat of high brain functions uses a six layer distribution of minicolumnar neurons to coordinate the integration of sensory information and the selection of relevant signals for goal driven behavior. To reveal the complex functionality of these columnar microcircuits we employed simultaneous recordings with several configurations of biomorphic microelectrode arrays (MEAs) within cortical layers in adjacent minicolumns, in four nohuman primates (NHPs) performing a delayed match-to-sample (DMS) visual discrimination task. We examined: 1) the functionality of inter-laminar, and inter-columnar interactions between pairs of cells in the same or different minicolumns by use of normalized cross-correlation histograms (CCH), 2) the modulation of Glutamate concentration in layer 2/3, and 3) the potential interactions within these microcircuits. The results demonstrate that neurons in both infra-granular and supra-granular layers interact through inter-laminar loops, as well as through intra-laminar to produce behavioral response signals. These results provide new insights into the manner in which prefrontal cortical microcircuitry integrates sensory stimuli used to provide behaviorally relevant signals that may be implemented in brain computer/machine interfaces (BCI/BMIs) during performance of the task.

Keywords

prefrontal cortex; executive control; columnar processing; microcircuits; glutamate modulation; nonhuman primates

[*]*Corresponding Author: Dr. Sam A. Deadwyler* and Dr. Ioan Opris, Wake Forest University School of Medicine, Department of Physiology and Pharmacology, Medical Center Boulevard, Winston Salem NC 27157, ph: 336-716-8540, fax: 336-716-8628, sdeadwyl@wfubmc.edu and *ioopris@wfubmc.edu*.

Introduction

The prefrontal cortex (PFC) located at the top of sensory-motor processing hierarchy (Fuster, 2001, Alexander et al., 1986) has been traditionally viewed as the seat of higher cognitive functions such as working memory, decision making and executive control of behavior (Fuster and Alexander, 1971; Funahashi et al., 1989; Miller 2000). Prefrontal cortical mechanisms of executive function, as outlined by the theories of cognition, coordinate and control 'online' cognitive processes involving memory storage, behavioral selection and motor planning (Baddeley 2002; Goldman-Rakic 1996; Graybiel 2008; Miller & Cohen 2001; Miyaki et al., 2000; Posner & Snyder 1975; Shallice & Burgess 1996). Prefrontal neural activity emerging from cortical layers and minicolumns is hypothesized to play a critical role to integrate sensory information and to select signals for goal driven behavior (Baddeley 2002; Goldman-Rakic 1996; Miller & Cohen 2001; Mountcastle 1997; Rao et al., 1999; Casanova et al., 2007, 2009).

Cortical minicolumns consist of vertically-oriented "modules" of cell bodies that represent the basic anatomic and physiologic microcircuitry of the cerebral cortex (Mountcastle 2003) that consist of pyramidal cells and several types of GABAergic, inhibitory interneurons (i.e. double-bouquet, basket and chandelier cells) (Sokhadze et al., 2012; Casanova 2007; Casanova et al. 2002a,b). Minicolumns in PFC are interconnected to each other through horizontal "long range" projections in layer 2/3 (Kritzer & Goldman-Rakic, 1995), inter-laminar mini-loops (Weiler et al., 2008; Takeuchi et al., 2011) and "reverberatory loops" through projections to the subcortical basal ganglia nuclei and thalamus (Alexander et al., 1886). Such "reverberatory loops" combine incoming signals from thalamus in layer 4 and inputs from cortical horizontal projections in layer 2/3, in order to compare inputs to a threshold criterion triggering an output response under specific conditions. Each layer, however, has also "short-range" projections involving inter-neurons in local circuit operations within cortical layers. However, understanding the modulation of firing between the two prefrontal cortical layers is now becoming necessary to perfect analyses and build brain computer interfaces (BCIs) for a broad range of cortically-related disorders (Lebedev and Nicolelis, 2006; Opris, 2013).

To address this necessity, we recorded simultaneously firing patterns of cells (from PFC area 46, 8 and 6) along cortical minicolumns (using W1 type MEAs) and between prefrontal cortical layers using custom designed multi-electrode-arrays that allowed simultaneous recording from both layers on adjacent minicolumns in four nonhuman primates (NHPs) performing a delayed match-to-sample (DMS) visual discrimination task. Results presented bellow provide new insights into the functionality of inter-laminar, intra-laminar and inter-columnar interactions between pairs of cells in the same or different layer/minicolumn by use of normalized cross-correlation (CCH) for short-lag CCHs that characterize short range interactions, and for longer CCHs that characterize more persistent interactions. In addition the modulation of Glutamate concentration in the layer 2/3 of prefrontal cortical cortex using similar MEAs was assessed under the same behavioral task conditions to correlate with columnar processing demonstrated under similar conditions. The results are relevant for the implementation of cortical microcircuits in BCI/BMIs.

METHODS

All animal procedures were reviewed and approved by the Institutional Animal Care and Use Committee of Wake Forest University, in accordance with U.S. Department of Agriculture, International Association for the Assessment and Accreditation of Laboratory Animal Care, and National Institutes of Health guidelines.

Visual Delayed-Match-to-Sample (DMS) Task

The NHPs utilized as subjects in this study (n=4) were trained for 2 or more years to perform the well characterized, custom-designed visual delayed-match-to-sample (DMS) task used in many prior studies (Opris et al., 2011; Hampson et al., 2011) shown in Fig. 1a. Animals were seated in a primate chair with a platform in front of a display screen in which position of the arm on the platform was tracked via a UV-fluorescent reflector affixed to the wrist, illuminated via a 15 W UV lamp, and detected by an LCD camera positioned 30 cm above. Hand position and movement was displayed as a bright yellow cursor on the screen and position of illuminated clip-art images computed from the video image using a Plexon Cineplex scanner. The DMS task paradigm is shown in Figure 1a. Trials were initiated by the animal placing the cursor inside a yellow 3” circle or square randomly illuminated in one of the 9 spatial positions on the screen. The presence of either the circle or square constituted the “Start” signal for the trial and indicated the “trial type” with respect to the Match-reward contingency on the same trial (Fig. 1a). Placement of the cursor into the Start signal image produced a trial unique clip-art image randomly displayed in one of 8 peripheral screen positions on each trial for 2,0s, which characterized the “Sample Phase” of the task. Movement of the cursor into the Sample image (Sample Response) blanked the screen and initiated the Delay phase for 10-60s, randomly presented on different trials in the session. The timeout of the Delay interval initiated the onset of the Match phase of the task (Match”) in which the Sample image and 2–7 trial unique ‘distracter’ clip-art images, were presented on the screen with position selected randomly on each trial. Placement of the cursor into either, 1) the Sample image (red arrow-*Object* trial) or 2) the same location as the prior Sample Response (blue arrow-*Spatial* trial), on the Match phase screen constituted the correct “Match Response (MR)” which produced a drop of juice delivered via a sipper tube near the animal's mouth, and blanked the screen for 10s until the next trial. Placement of the cursor into a different (non-match) distracter image on an *Object* trial, or into a different spatial location than where the Sample image was responded to as required on a *Spatial* trial, constituted a MR error that blanked the screen without reward delivery and initiated the 10s inter-trial interval (ITI). All clip-art images (sample and distracter) were unique for each trial in all daily sessions of 100-150 trials, due to random selection from a 10,000 image selection buffer which was updated monthly. The 4 NHPs were trained to overall performance levels of 70-75% correct with respect to the above described DMS task parameters (Fig 1b).

Surgery

Animals were surgically prepared with cylinders for attachment of a microelectrode manipulator over the specified brain regions (Fig. 1c) where recordings were made in this study.. During surgery animals were anesthetized with ketamine (10 mg/kg), then intubated

and maintained with isoflurane (1-2 % in oxygen 6 l/min). Recording cylinders (Crist Instruments, Hagerstown, MD) were placed over 20 mm diameter craniotomies positioned via stereotaxic coordinates for electrode access to the Frontal Cortex (25 mm anterior relative to interaural line and 12 mm lateral to midline/vertex) in the caudal region of the Principal Sulcus. Access to the dorsal limb of Arcuate Sulcus in area 8 and the dorsal part of premotor area 6 (Hampson et al., 2011), areas were previously shown by PET imaging to be activated during task performance (Hampson et al., 2009). Two titanium posts were secured to the skull for head positioning during task performance. Following surgery, animals were given 0.025 mg/kg buprenorphine for analgesia and penicillin to prevent infection. Recording cylinders were disinfected thrice weekly with Betadine during recovery and daily during recording.

Electrophysiology: Recording and Stimulation

Electrophysiological procedures and analysis utilized the Plexon MAP Spike Sorter (Dallas, TX) for 64 channel simultaneous recordings. All customized conformal designed ceramic multielectrode arrays (MEAs) were constructed by Dr. Greg Gerhardt with at University of Kentucky, Center for Microelectrode Technology – CenMet, Lexington, KY, and consisted of etched platinum pads (Fig. 2 a-c) designed via collaboration for recording multiple single neuron activity in specific brain regions (Hampson et al., 2004, 2011). Single extracellular action potentials were isolated and analyzed with respect to activity on specific recording pads (impedance range 0.5-3.0 MOhms) during different events within DMS trials. The configuration of the MEA (Fig. 2 a-c**)** was specially designed to conform to the columnar anatomy of the PFC such that the top 4 recording pads recorded activity from neurons in the supra-granular layer 2/3 (L2/3) while the lower set of four pads (Fig. 1d), separated vertically by 1350 μm, simultaneously recorded neuron activity in the infra-granular layer 5 (L5) of the PFC. In order to study the 3-dimensional columnar-laminar organization of the cortex we can use multiple MEAs (4 to 16 arrays) for PFC recordings and 4 MEAS for hippocampal recordings.

Electrochemical Recording

Ceramic MEAs similar to those utilized above (Fig. 2) for electrophysiological recording were also prepared for electrochemical recording (Fig. 6; Burmeister et al. 2004, 2008; Quintero et al. 2007, 2011; Hascup et al. 2008, 2011; Fuqua et al. 2010). The electrochemistry arrays consisted of four recording sites (15 × 333 μM) in two rows, separated by 500 μm, with a 7 cm polyimide shaft for depth positioning. The electrodes were configured to record from Layer 2/3 with the reference in Layer 1. MEAs were dip coated with Nafion®, a fluoropolymer which excludes the passage of anions, thus ensuring that only cations would reach the platinum recording surface. The dorsal (“sentinel” or reference) recording sites were coated with bovine serum albumin (BSA) plus glutaraldehyde; ventral recording sites were coated with Glutamate oxidase and BSA + glutaraldehyde. The GluOx coating allowed the ventral pads to be sensitive to glutamate release through the enzymatic production of H_2O_2. A +0.7V charging potential was applied to the MEA once per second (using an Ag/AgCl reference electrode) to oxidize the H_2O_2 resulting from detection of glutamate at the electrode. The “relaxation” current from H_2O_2

oxidation was proportional to second-by-second changes in glutamate concentration at the electrode (Quintero et al. 2011).

Data Analysis

Task performance was determined for each animal (n=4) as percent correct trials within and across sessions and related to simultaneous MEA recordings on individual trials during Match phase image selection (MR) in the task (Hampson et al., 2011). Cell types were identified as regular firing pyramidal cells in terms of baseline (nonevent) firing rate (Opris et al., 2009) and significant changes ($z > 3.09$, $p < 0.001$) in firing (see below) on single trials in perievent histograms (PEHs) derived for intervals of ± 2.0s relative to the time of Match screen presentation that signaled onset of the Match phase of the task (Fig. 2,3). Task-related neural activity was classified according to locations on the biomorphic MEA positioned specifically in L2/3 and L5 (Fig. 2) upon insertion in PFC prior to the start of the DMS session. To account for neuronal responses in terms of columnar microcircuit organization neurons recorded on the MEAs were characterized by 1) simultaneously detected cell activity on both sets of ve*rtical* separated (1350 μm) MEA pads (L2/3 cells on upper 4 pads, and L5 cells lower pads), during electrode positioning at the start of the session (Fig. 2 D-F) whether firing of the same cell pair on pads with the same vertical location on the MEA was modulated similarly during the Match phase of the DMS task (Hampson et al., 2012). Standard (Z) scores of increased firing rates relative to nonevent baseline values were calculated for individual cells for each DMS task event. Firing rate was analyzed in 250 ms bins for ± 2.0 s relative to time of initiation (0.0s) task events. Only neurons with firing rates significantly elevated from that in pre-event phases (−2.0 to 0.0s) baseline period were included for analysis. Differences in cross-correlation between neuron spikes of L2/3 and L5 cell pairs on the same vertical alignment on MEA pads (Fig 2B&C, Fig 2E&F) were assessed for the same temporal intervals using standardized distributions of correlation coefficients assessed under different conditions related to performance in the Match Phase (Figs. 4 and 5). Scatter plots compared normalized CCHs coefficients relative to time lag of synchronized firing for the same populations of cell pairs under different experimental conditions (Fig. 5), all of which satisfied a 99% confidence requirement (Opris et al., 2011). CCHs were generated using a shift predictor algorithm (NeuroExplorer) (http://www.neuroexplorer.com/), which computed chance cross-correlation levels by randomizing the actual spike sequence and calculating cross-correlations 5 different times for a given pair of neurons, which was then subtracted from the task derived coefficients for CCHs to adjust for correlated firing due to differences in cell firing rates and/or frequency of bursting (Opris et al., 2011; Takeuchi et al., 2011). Population CCHs, were computed across individual cell CCHs, normalized as a function of probability, by averaging coefficients across multiple cell pairs and plotting the mean values (±SEM) in 1.0 ms bins.

Identification of Cortical Layers and Minicolumns

The neuromorphic MEAs (model W2 and W3, Fig. 2 B&C**)** were designed so that the two sets of recording pads could only record simultaneous activity from neurons separated by ~600 μm (for W2), 1350 μm (W3), which given the orientation of insertion into PFC perpendicular to cell layers, could only consist of infra-granular layer 5 and supra-granular layer 2/3 cell activity recorded at the same time as a function of placement depth of MEA

(Opris et al., 2011;Takeuchi et al., 2011; Hansen & Dragoi, 2011). Model W1 (Fig. 2A), in addition to supra- and infra-granular layers allowed recording in granular layer 4, as well. Misplacement of the W2/W3 probes due to a different angular penetration relative to columnar orientation in PFC was detectable by the absence of simultaneous cell recordings on the sets of vertically separated (600 and 1350 μm) pads. In addition, the MEAs (Opris et al., 2011; Hampson et al., 2004) employed here allowed simultaneous recording of two adjacent PFC minicolumns (Fig. 2A-C) since, activity from adjacent minicolumns could be detected, since MEA pads were separated laterally by 40μm which exceeds the distances reported (28μm) via anatomic assessments (Casanova et al., 2009).

Results

Four nonhuman primate (NHP) subjects (Macaca mulatta rhesus) were trained to perform a delayed-match-to-sample (DMS) task with instructions to select the image (object) or the spatial location of the image (spatial) presented in the prior Sample phase from a set of 2-7 distracter images in the Match Phase after an intervening Delay of 1-50 sec (Fig. 1a). NHPs made hand tracking movements to visual targets presented on the screen in front of them to obtain a juice reward for selection of the correct (Sample) image. The key variables in the task were the number of distracter images and the duration of the delay (1 to 50 sec) presented randomly on single trials in sessions with 100-150 trials.

A. Neural recordings of cortical layers and minicolumns with neuromorphic MEAs

New approaches to the study of columnar/laminar microanatomy/microcircuitry and functionality of the brain have emerged recently (Opris et al., 2011, 2012a, 2012b; 2013; Constantinople and Bruno, 2013, Hansen et al, 2012 Takeuchi et al., 2011, Mahan and Georgopoulos, 2013). Among most effective recent microelectrode technologies, the neuromorphic ceramic-based multisite electrode arrays (MEAs) are instrumental for in vivo single-neuron recording (Moxon et al. 2004) both in neocortical and hippocampal neurons of rodents and primates. Figure 2 D-F shows examples of recorded cells with the configuration of neuromorphic arrays of type W1-W3 (Fig. 2 A-C). On can easily distinguish neurons from supra-granular (blue) or infra-granular (pink) layers, as well as cells from the granular (green) layer. A major feature of these MEAs resides in the fact that they allow us to get insight into the functional microanatomy of cortical layers and minicolumns in order to trace the cognitive processing of inter-laminar microcircuits.

B. Multi-functional firing of neurons in cortical layers and minicolumns

Prefrontal cortical cells have been implicated in a variety of cognitive functions, including the multi-functional (multitasking) neurons that may enable efficient monitoring and control of ongoing behaviors that depend on attention, working memory and target selection. Figure 3 shows the differential firing of two neurons from layer 2/3 (upper panel) and layer 5 (lower panel), on spatial or object type (Fig. 3A&B; See also Opris et al., 2013) and correct and error trials (Fig. 3C; See also Opris et al., 2012a). Also, during target selection the layer 2/3 cell fires higher on correct trials than on error trials (Fig 3C). These results reveal the multi-functional ability of prefrontal cortical microcircuits.

C. Complex microcircuitry between cortical layers and minicolumns

Columnar-laminar microcircuits in prefrontal cortex have a complex interactive routine as shown in Figure 4, including inter-laminar (Fig. 4A) and inter-columnar (Fig. 4B) interactions that are extracted by constructing cross-correlation histograms (CCHs) for each cell pair to be compared Hampson et al 2012, Opris et al 2013). These types of inter-laminar interactions were sensed by biomorphic MEAs (Fig 4A) positioned to simultaneously record neurons in layers 2/3 and layer 5 in adjacent “columns” during all phases of the DMS task. Figure 4C shows inter-columnar interactions with long range connections from other subcortical structures (McFarland and Haber, 2002; Opris et al., 2011, 2012ab, 2013; Constantinople & Bruno, 2013). In addition, the direct interaction between different minicolumns is faster or “short ranged” and in some cases bilateral (Zhang and Alloway, 2006) as shown in Fig. 4B.

A typical “long lag” cross-correlation histogram for a layer 5 cell pair separated by 100 μm on the MEA, has a broad peak at 100 ms lag (Fig. 5A). In Figure 5B is shown the distribution of cross-correlation peaks as a function of temporal lag for inter-layer CCHs (red; n=154 pairs) and intra-layer CCHs (blue; n=56 pairs). The normalized CCHs (Opris et al., 2012a,b) show the probability of synchronized firing of layer 5 cells within ± 150.0 ms of individual spike occurrences from the layer 2/3 cell (0 ms in CCH). Similarly, the distribution of short lagged CCHs (Fig. 5C) is shown in Fig 5D. The CCH in Fig. 5C provides evidence for common input on both cells of the pair and direct input from left to right cell. The distribution of the intra-layer (blue; n=60 cells) cross-correlation peaks as a function of temporal lag indicates the existence of inter-laminar mini loops.

It is becoming clear that the pairs of cells that showed high correlated firing between layers are part of the complex intra-laminar and thalamo-cortical reverberatory loops involved in the cognitive function of prefrontal cortex (Swadlow and Gusev, 2002; Salinas et al. 2000; Constantinople and Bruno, 2013).

D. Glutamatergic modulation of prefrontal cortical microcircuitry

The excitatory inputs from glutamate neurotransmission have been intimately involved in learning and memory (Hascup et al., 2008, 2011). The ability to evoke glutamate release events is necessary to investigate the glutamate's role in learning and memory. Performance of the DMS task was examined for release of glutamate within NHP prefrontal cortex. After glutamate sensor biomorphic MEAs (Figure 6) were placed in layer 2/3 of PFC, basal glutamate concentrations, number of glutamate release events, and the change in glutamate concentration were analyzed in relation to emission within different the phases of the DMS task (Opris et al., 2012b; Hampson et al., 2013b). Figure 6A shows the MEA used to record Glutamate from PFC layer 2/3 (Fig. 6B) in nonhuman primates.

Tonic glutamate levels (Fig. 6C,D) were shown to increase significantly ($p<0.001$; ANOVA) in the Match (decision) phase of DMS task for both Spatial and Object trials, while increased transient glutamate release (frequency) increased in the Sample (encoding) phase of the task (Fig. 6E,F). In addition, spatial vs. object DMS trials evoked differential changes ($p<0.001$; ANOVA) in glutamate amplitude levels (Fig. 6G&H). The tonic vs.

phasic % change in glutamate concentration and frequency of events is compared in by scatter plots in Fig. 6I&J.

DISCUSSION

Our results provide new and detailed insights into the manner in which prefrontal cortical microcircuit integrates sensory stimuli used to provide behaviorally relevant signals during the execution of the task. On the other hand, recordings from prefrontal cortex with biomorphic MEAs, which reveals complex columnar-laminar microcircuits, allows not only to understand how the brain performs cognitive processing, but, also, to think about potential applications to brain neuroprosthetics and interfaces of the brain with computer (BCI) or a machine (BMI). Some of this is reviewed below with respect to: a) the role of biomorphic MEAs in electrophysiological and electrochemical recordings, b) the complexity and multitasking functionality of microcircuits, c) the glutamatergic modulation, and d) their direct implication for the design of future BCI and BMI.

a. Neuromorphic ceramic probes for electrophysiology and electrochemistry

The neuromorphic probes were recently employed to record neural activity and glutamatergic dynamics of prefrontal cortical activity involved in perception, working memory and executive control of behavior that emerges from operation of columnar-laminar microcircuits. Prefrontal cortical cell layers 2/3 are hypothesized to participate in temporal long-range supra-granular laminar circuit operations using horizontal convergent synaptic connections from cortical sensory areas. Inter-laminar microcircuits with layer 5 cells play key roles in the selection of behaviorally relevant stimuli as well as in short-range or local circuit operations within cortical layers. The inter-laminar signals are conveyed to the sub-cortical structures controlling behavioral response selection via reverberatory thalamo-cortical loops (Swadlow and Gusev, 2002; Salinas et al. 2000; Constantinople and Bruno, 2013).

It was then examined the interactions between cells of the same/different layer by use of cross-correlation with binsize = 0.1 ms (short-lag interactions), and long-lag interactions with cross-correlations in a binsize =1 and 5ms. As shown in Figs 4&5, these analyses dissociated neural firing in supra-granular, granular and infra-granular layers. The interaction between cells appears as inter-laminar (Fig. 4A) or inter-columnar (Fig. 4B) indicated by short lag CCHs (inter-laminar loops) and long lag CCHs (likely thalamo-cortical reverberatory loops). Our results point to a broad spectrum of interactions involving neurons from both infra-granular and supra-granular layers showing cross-correlations characteristic of inter-laminar loops, as well as long-range feed-forward or thalamo-cortical loops. These interactions reflect the involvement of cortical modules in the integration of stimuli in the supra-granular layers that integrate sensory signals and biases for goal driven behavior (Opris et al., 2011, 2013). Furthermore, to capture the causal relationships between these minicolumns the use of Dynamic Bayesian Networks (Smith et al., 2006) and Granger Causality (Granger, 1969) will help to infer the complex flow of neural signals involving these microcircuits.

In order to fully study the 3-dimensional columnar organization of the cortex, obviously it is required to use multiple electrode arrays in a small area to cover a patch of the cortex. A nontrivial aspect for future implementation in BCI/BMI relates to the limitation of MEAs density i.e. the smallest distance between arrays that may be compatible with cortical tissue. In an attempt to demonstrate MEAs feasibility, prefrontal cortical cells were recorded with 2 MEAs and in hippocampus with 4 MEAs, separated by 2 mm from each other (Hampson et al., 2013a ; Opris et al., 2014). Nevertheless, a probe with 16 MEAs (128 channels) having 1-2 mm separation between MEAs seems feasible in terms of scalability for future implementation in BCI/BMI.

b. Multitasking microcircuits

The prefrontal cortex has been implicated in a variety of cognitive functions, including working memory, attention, response inhibition, self-monitoring, motor planning, rule implementation, reward estimation, and decision making (Fuster, 2000; Miller and Cohen, 2001; Schall et al., 2002; Passingham and Sakai, 2004; Johnston and Everling, 2006; Muhammad et al., 2006; Champod and Petrides, 2007; Lee et al., 2007; Tanji and Hoshi, 2008). The multitasking neurons in PFC may enable efficient monitoring and control of ongoing behaviors that depend on both working memory and attention. For example, during a visual search, multitasking neurons may help distinguish locations that have previously been searched from those that need scrutiny. In general, the presence of multitasking neurons suggests a strategy by which the prefrontal cortex can efficiently represent different cognitive attributes of a given location and selectively access any such attribute depending on the behavioral context (Messinger et al., 2002).

c. Glutamate Modulation

Conformal ceramic electrodes were used in this study to record tonic glutamate concentration and transient release in PFC layer 2/3. Tonic glutamate concentration increased in the Match (decision) phase of the DMS task, while increased transient glutamate release occurred mostly in the Sample (encoding) phase of the task. Further, spatial vs. object-oriented DMS trials evoked differential changes in PFC layer 2/3 glutamate concentration. Thus the same conformal recording electrodes were capable of electrophysiological and electrochemical recording, which revealed similar evidence of event specific neural processing in layers 2/3 and layer 5 during cognitive processing in a behavioral task.

d. Implications for the design of BCI/BMI

A major advance provided by the modularity approach is the fine manipulation of the columnar microcircuits in the prefrontal cortex that can be implemented in BCI/BMI. Future BCI/BMIs seem to have a broad applicability from patients who suffered from stroke or have memory deficit to people with various executive dysfunctions. With the advance of nanotechnology (Vidu et al., 2014) nano-neuro-chips may be designed and be implanted in the prefrontal cortex of humans to repair the dysfunctions of cortical microcircuits (Opris, 2013). BCI/BMI may potentially improve cognitive performance, as it was already demonstrated in nonhuman primates (Opris et al., 2012a,b; Hampson et al 2012, 2013b). As shown by Steven Wise's team (Messenger et al., 2002) multitasking neurons in prefrontal

cortex may increase the degrees of freedom of a BCI/BMI, while keeping the same number of microelectrodes. This and other advantages may recommend multi-functional (multitasking) neurons as potential candidates for BCI/BMI. The BCI/BMIs with columnar architecture may be implemented by microchips implanted in the cortex and activated by a wireless controller. Moreover, changes in the normal functioning of the columnar microcircuits can help the understanding of different mental disorders and BCI/BMIs can help in the rehabilitation of the patients. Nevertheless, our previous work has shed light into the enhancement of cognitive performance by means of patterned microstimulation (Hampson et al., 2012, 2013b, Deadwyler et a., 2014).

In summary, these unique results show that columnar relations between prefrontal neurons that encode and process information relevant to executive function and decision making (target/response selection) are necessary for successful task performance (Fig 2) and are the factors responsible for disrupted cognition in neurological and psychiatric disorders. The actual neural basis for effective performance in this task therefore relates to the significant correlation between PFC layer 2/3 and layer 5 cell activity during target presentation by a microcircuit that provides the “selection bias” emerging from similar spatially tuned responses (i.e. inter-laminar correlated firing) during the decision phase of the task. Moreover, given this effect on glutamatergic substrates, the modulation in inter-laminar firing provides insight into an entire spectrum of cognitive functions, which has proven critical for initial investigations involved in the use of neuroprostheses (BCI/BMIs) for repairing impairments related to disrupted cortical function in primate brain (Hampson et al 2012; Opris et al., 2012a,b).

Acknowledgment

We thank Josh Long, Joe Noto, Brian Parish, Shahina Koshisseri, Joshua Fuqua, Mack Miller and for their assistance on this project. This work was supported by National Institutes of Health Grants DA06634, DA023573, DA026487 and by Defense Advanced research Projects Agency (DARPA) contract N66601-09-C-2080 to S.A.D.

REFERENCES

Baddeley, A. Fractionating the central executive.. In: Stuss, DT.; Knight, RT., editors. Principles of Frontal Lobe Function. Oxford University Press; New York: 2002. p. 246-260.

Brennan AR, Arnsten A. Neuronal mechanisms underlying attention deficit hyperactivity disorder: the influence of arousal on prefrontal cortical function. Ann NY Acad Sci. 2008; 1129:236–245. [PubMed: 18591484]

Buffalo EA, Fries P, Landmanc R, Buschman TJ, Desimone R. Laminar differences in gamma and alpha coherence in the ventral stream. Proc Natl Acad Sci USA. 2011; 108:11262–67. [PubMed: 21690410]

Burmeister JJ, Coates TD, Gerhardt GA. Multisite microelectrode arrays for measurements of multiple neurochemicals. Conf Proc IEEE Eng Med Biol Soc. 2004; 7:5348–5351. [PubMed: 17271550]

Burmeister JJ, Pomerleau F, Huettl P, Gash CR, Werner CE, Bruno JP, Gerhardt GA. Ceramic-based multisite microelectrode arrays for simultaneous measures of choline and acetylcholine in CNS. Biosens Bioelectron. 2008; 23:1382–1389. [PubMed: 18243683]

Buxhoeveden DP, Casanova MF. The minicolumn hypothesis in neuroscience. Brain. 2002; 125:935–951. [PubMed: 11960884]

Casanova MF, Buxhoeveden DP, Cohen M, Switala AE, Roy EL. Minicolumnar pathology in dyslexia. Ann Neurol. 2002a; 52(1):108–10. [PubMed: 12112057]

Casanova MF, Buxhoeveden DP, Brown C. Clinical and macroscopic correlates of minicolumnar pathology in autism. J Child Neurol. 2002b; 17(9):692–695. [PubMed: 12503647]

Casanova MF, Buxhoeveden D, Gomez J. Disruption in the inhibitory architecture of the cell minicolumn: implications for autism. Neuroscientist. 2003; 9(6):496–507. [PubMed: 14678582]

Casanova MF, Switala AE, Trippe J, Fitzgerald M. Comparative minicolumnar morphometry of three distinguished scientists. Autism. 2007; 11(6):557–569. [PubMed: 17947291]

Casanova, et al. Neuronal distribution in the neocortex of schizophrenic patients. Psychiatry Research. 2008; 158:267–277. [PubMed: 18280583]

Casanova, et al. Minicolumnar width: Comparison between supragranular and infragranular layers. J Neurosci. Methods. 2009; 184:19–24. [PubMed: 19616026]

Constantinople CM, Bruno RM. Deep cortical layers are activated directly from thalamus. Science. 2013; 340:1591–1594. [PubMed: 23812718]

Deadwyler SA, Porrino L, Siegel JM, Hampson RE. Systemic and nasal delivery of orexin-A (Hypocretin-1) reduces the effects of sleep deprivation on cognitive performance in nonhuman primates. J Neurosci. 2007; 27(52):14239–47. [PubMed: 18160631]

Deadwyler SA, Berger TW, Sweatt AJ, Song D, Chan RH, Opris I, Gerhardt GA, Marmarelis VZ, Hampson RE. Donor/recipient enhancement of memory in rat hippocampus. Front Syst Neurosci. Dec 26.2013 7:120. doi: 10.3389/fnsys.2013.00120. eCollection 2013. [PubMed: 24421759]

Dobbs D. Schizophrenia: The making of a troubled mind. Nature. 2010; 468:154–156. [PubMed: 21068803]

Dudkin KN, Chueva IV, Arinbasarov MU, Bobkova NV. Organization of working memory processes in monkeys: the effects of a dopamine receptor agonist. Neurosci Behav Physiol. 2003; 33:387–398. [PubMed: 12774842]

Duncan J, Johnson R, Swales M, Freer C. Frontal lobe deficits after head injury: Unity and diversity of function. Cognitive Neuropsychology. 1997; 14:713–741.

Felsen G, et al. Dynamic modification of cortical orientation tuning mediated by recurrent connections. Neuron. 2002; 36:945–954. [PubMed: 12467597]

Fuqua, JL.; Quintero, JE.; Long, JL.; Noto, JV.; Hampson, RE.; Gerhardt, GA.; Deadwyler, SA. 2010 Neuroscience Meeting Planner. Society for Neuroscience; Washington, DC: 2010. Electrical stimulation of glutamate release in the hippocampus.. Program No. 610.8

Fuster JM, Alexander GE. Neuron activity related to short-term memory. Science. 1971; 173:652–654. [PubMed: 4998337]

Fuster JM. The prefrontal cortex--an update: time is of the essence. Neuron. 2001; 30:319–33. [PubMed: 11394996]

Goldman-Rakic PS. The prefrontal landscape: implications of functional architecture for understanding human mentation and the central executive. Philos Trans R Soc Lond B Biol Sci. 1996; 351:1445–1453. [PubMed: 8941956]

Granger CWJ. Investigating causal relations by econometric models and cross-spectral methods. Econometrica. 1969; 37:424–438. doi: 10.2307/1912791.

Graybiel AM. Habits, rituals, and the evaluative brain. Annu Rev Neurosci. 2008; 31:359–387. [PubMed: 18558860]

Hascup KN, Hascup ER, Pomerleau F, Huettl P, Gerhardt GA. Second-by-second measures of L-glutamate in the prefrontal cortex and striatum of freely moving mice. J Pharmacol Exp Ther. 2008; 324:725–731. [PubMed: 18024788]

Hascup KN, Hascup ER, Stephens ML, Glaser PE, Yoshitake T, Mathe AA, Gerhardt GA, Kehr J. Resting glutamate levels and rapid glutamate transients in the prefrontal cortex of the Flinders Sensitive Line rat: a genetic rodent model of depression. Neuropsychopharmacology. 2011; 36:1769–1777. [PubMed: 21525860]

Heyselaar E, Johnston K, Paré M. A change detection approach to study visual working memory of the macaque monkey. J Vis. 2011; 11(3):11. doi: 10.1167/11.3.11. [PubMed: 21402883]

Hampson RE, Porrino LJ, Opris I, Stanford T, Deadwyler SA. Effects of cocaine rewards on neural representations of cognitive demand in nonhuman primates. Psychopharmacology (Berl). 2011; 213:105–118. [PubMed: 20865250]

Hampson RE, Coates TD Jr, Gerhardt GA, Deadwyler SA. Ceramic-based micro-electrode neuronal recordings in the rat and monkey. Proceedings of the Annual International Conference of the IEEE Engineering in Medicine and BIology Society (EMBS). 2004; 25:3700–3703.

Hampson RE, Gerhardt GA, Marmarelis VZ Song D, Opris I, Santos LM, Berger TW, Deadwyler SA. Facilitation and Restoration of Cognitive Function in Primate Prefrontal Cortex by a Neuroprosthesis that Utilizes Minicolumn-Specific Neural Firing. J Neural Eng. 2012; 9:056012. doi:10.1088/1741-2560/9/5/056012. [PubMed: 22976769]

Hampson RE, Fuqua JL, Huettl PF, Opris I, Song D, Shin D, Marmarelis VZ, Berger TW, Gerhardt GA, Deadwyler SA. Conformal ceramic electrodes that record glutamate release and corresponding neural activity in primate prefrontal cortex. Conf Proc IEEE Eng Med Biol Soc. 2013a; 2013:5954–7. doi: 10.1109/EMBC.2013.6610908. [PubMed: 24111095]

Hampson RE, Song D, Opris I, Santos LM, Shin DC, Gerhardt GA, Marmarelis VZ, Berger TW, Deadwyler SA. Facilitation of memory encoding in primate hippocampus by a neuroprosthesis that promotes task-specific neural firing. J Neural Eng. Dec.2013b 10(6):066013. doi: 10.1088/1741-2560/10/6/066013. [PubMed: 24216292]

Hansen B, Dragoi V. Adaptation-induced synchronization in laminar cortical circuits. Proc Natl Acad Sci USA. 2011; 108:10720–10725. [PubMed: 21659632]

Heekeren HR, Marrett S, Ungerleider LG. The neural systems that mediate human perceptual decision making. Nat Rev Neurosci. 2008; 9(6):467–479. [PubMed: 18464792]

Hong S, Ratté S, Prescott SA, De Schutter E. Single Neuron Firing Properties Impact Correlation-Based Population Coding. J Neurosci. 2012; 32(4):1413–1428. [PubMed: 22279226]

Kritzer MF, Goldman-Rakic PS. Intrinsic circuit organization of the major layers and sublayers of the dorsolateral prefrontal cortex in the rhesus monkey. J Comp Neurol. 1995; 359:131–143. [PubMed: 8557842]

Kelley TA, Lavie N. Working memory load modulates distractor competition in primary visual cortex. Cereb Cortex. 2011; 21(3):659–665. [PubMed: 20699229]

Lebedev MA, Nicolelis MAL. Brain-machine interfaces: past, present and future. Trends Neurosci. 2006; 29:536–546. [PubMed: 16859758]

Lund JS, Angelucci A, Bressloff PC. Anatomical substrates for functional columns in macaque monkey primary visual cortex. Cereb Cortex. 2003; 13(1):15–24. [PubMed: 12466211]

Mahan MY, Georgopoulos AP. Motor directional tuning across brain areas: directional resonance and the role of inhibition for directional accuracy. Front. Neural. Circuits. 2013; 7:92. doi:10.3389/fncir.2013.00092. [PubMed: 23720612]

McFarland NR, Haber SN. Thalamic relay nuclei of the basal ganglia formboth reciprocal and nonreciprocal cortical connections, linking multiple frontal cortical areas. J. Neurosci. 2002; 22(18):8117–8132. [PubMed: 12223566]

Messinger A, Lebedev MA, Kralik JD, Wise SP. Multitasking of attention and memory functions in the primate prefrontal cortex. J Neurosci. 2002; 2929(17):5640–53. [PubMed: 19403830]

Meyer T, Qi XL, Stanford TR, Constantinidis C. Stimulus selectivity in dorsal and ventral prefrontal cortex after training in working memory tasks. J Neurosci. 2011; 31(17):6266–76. [PubMed: 21525266]

Miller EK, Cohen JD. An integrative theory of prefrontal cortex function. Annu Rev Neurosci. 2001; 24:167–202. [PubMed: 11283309]

Miyaki A, Friedman N, Emerson M, Witzki A, Howerter A, Wagner T. The unity and diversity of executive functions and their contributions to complex frontal lobe tasks: A latenet variable analysis. Cog Psychol. 2000; 41:49–100.

Mo J, Schroeder CE, Ding M. Attentional modulation of alpha oscillations in macaque inferotemporal cortex. J Neurosci. 2011; 31(3):878–882. [PubMed: 21248111]

Mountcastle VB. The columnar organization of the neocortex. Brain. 1997; 120(4):701–722. [PubMed: 9153131]

Nicolelis MA, Dimitrov D, Carmena JM, Crist R, Lehew G, Kralik JD, et al. Chronic, multisite, multielectrode recordings in macaque monkeys. Proc. Natl. Acad. Sci. U.S.A. 2003; 100:11041–11046. [PubMed: 12960378]

Opris I, Barborica A, Ferrera VP. Comparison of performance on memory-guided saccade and delayed spatial match-to-sample tasks in monkeys. Vision Research. 2003; 43:321–332. [PubMed: 12535990]

Opris I, Barborica A, Ferrera VP. A gap effect during micro-stimulation in the prefrontal cortex of monkey, Exp. Brain Res. 2001; 138:1–7.

Opris I, Barborica A, Ferrera VP. Comparison of performance on memory-guided saccade and delayed spatial match-to-sample tasks in monkeys. Vision res. 2003; 43(3):321–32. [PubMed: 12535990]

Opris I, Barborica A, Ferrera VP. Microstimulation of Dorsolateral Prefrontal Cortex Biases Saccade Target Selection. J Cogn Neurosci. 2005a; 17:893–904. [PubMed: 15969908]

Opris I, Barborica A, Ferrera VP. Effects of Electrical Microstimulation in Monkey Frontal Eye Field on Saccades to Remembered Targets. Vision Research. 2005b; 45:3414–3429. [PubMed: 15893784]

Opris I, Bruce CJ. Neural circuitry of judgment and decision mechanisms. Brain Res Rev. 2005; 48:509–526. [PubMed: 15914255]

Opris I, Hampson RE, Stanford TR, Gerhardt GA, Deadwyler SA. Neural activity in frontal cortical cell layers: evidence for columnar sensorimotor processing. J Cogn Neurosci. 2011; 23:1507–1521. [PubMed: 20695762]

Opris I. Lebedev MA, Opris I, Casanova MF. Inter-Laminar Microcircuits across the Neocortex: Repair and Augmentation. Frontiers in Systems Neuroscience Research Topic: “Augmentation of brain function: facts, fiction and controversy”. 2013 doi:doi: 10.3389/fnsys.2013.00080.

Opris I, Hampson RE, Gerhardt GA, Berger TW, Deadwyler SA. Columnar processing in primate prefrontal cortex: Evidence for executive control microcircuits. J Cogn Neurosci. 2012 in press, doi:10.1162/jocn_a_00307.

Opris I, Fetterhoff D, Sexton CA, Santos LM, Long JL, Parish BC, Noto JV, Jurchescu OD, Enachescu M, Gerhardt GA, Song D, Marmarelis VZ, Berger TW, Hampson RE, Deadwyler SA. Integration of Executive Control Signals Across Prefrontal Cortical-Striatal and Hippocampal CA1-CA3 Neural Ensembles. SFN Abstracts. 2014

Pesaran B, Nelson MJ, Andersen RA. Free choice activates a decision circuit between frontal and parietal cortex. Nature. 2008; 453:406–409. [PubMed: 18418380]

Porrino LJ, Daunais JB, Rogers GA, Hampson RE, Deadwyler SA. Facilitation of task performance and removal of the effects of sleep deprivation by an ampakine (CX717) in nonhuman primates. PLoS Biol. 2005; 3(9):e299. [PubMed: 16104830]

Posner, M.; Snyder, C. Attention and cognitive control.. In: Solso, R., editor. Information Processing and Cognition: The Loyola Symposium. L. Erlbaum Assoc.; Hillsdale, NJ: 1975.

Rao SG, Williams GV, Goldman-Rakic PS. Isodirectional tuning of adjacent interneurons and pyramidal cells during working memory: evidence for microcolumnar organization in PFC. J Neurophysiol. 1999; 81:1903–1916. [PubMed: 10200225]

Resulaj A, Kiani R, Wolpert DM, Shadlen MN. Changes of mind in decision-making. Nature. 2009; 461:263–266. [PubMed: 19693010]

Robbins TW, Arnsten AF. The neuropsychopharmacology of fronto-executive function: monoaminergic modulation. Annu Rev Neurosci. 2009; 32:267–287. [PubMed: 19555290]

Quintero JE, Day BK, Zhang Z, Grondin R, Stephens ML, Huettl P, Pomerleau F, Gash DM, Gerhardt GA. Amperometric measures of age-related changes in glutamate regulation in the cortex of rhesus monkeys. Exp Neurol. 2007; 208:238–246. [PubMed: 17927982]

Quintero JE, Pomerleau F, Huettl P, Johnson KW, Offord J, Gerhardt GA. Methodology for rapid measures of glutamate release in rat brain slices using ceramic-based microelectrode arrays: basic characterization and drug pharmacology. Brain Res. 2011; 1401:1–9. [PubMed: 21664606]

Riedel G, Platt B, Micheau J. Glutamate receptor function in learning and memory. Behav Brain Res. 2003; 140:1–47. [PubMed: 12644276]

Shepherd, G.; Grillner, S. Handbook of Brain Microcircuits. Oxford University Press; Oxford: 2010.

Shallice T, Burgess PW. Deficits in strategy application following frontal lobe damage in man. Brain. 1991; 114(2):727–741. [PubMed: 2043945]

Shallice T, Burgess P. The domain of supervisory processes and temporal organization of behaviour. Philos Trans R Soc Lond B Biol Sci. 1996; 351:1405–1411. [PubMed: 8941952]

Smith VA, Yu J, Smulders TV, Hartemink AJ, Jarvis ED. Computational inference of neural information flow networks. PLoS Comput. Biol. 2006; 2:e161. doi: 10.1371/journal.pcbi.0020161. [PubMed: 17121460]

Sokhadze EM, Baruth JM, Sears L, Sokhadze GE, El-Baz AS, Casanova MF. Prefrontal neuromodulation using rTMS improves error monitoring and correction function in autism. Appl Psychophysiol Biofeedback. 2012; 37(2):91–102. [PubMed: 22311204]

Stephens ML, Pomerleau F, Huettl P, Gerhardt GA, Zhang Z. Real-time glutamate measurements in the putamen of awake rhesus monkeys using an enzyme-based human microelectrode array prototype. J Neurosci Methods. 2010; 185:264–272. [PubMed: 19850078]

Sugrue LP, Corrado GS, Newsome WT. Choosing the greater of two goods: neural currencies for valuation and decision making. Nat Rev Neurosci. 2005; 6:363–375. [PubMed: 15832198]

Swadlow HA, Gusev AG, Bezdudnaya T. Activation of a cortical column by a thalamocortical impulse. J Neurosci. 2002; 22:7766–7773. [PubMed: 12196600]

Takeuchi D, Hirabayashi T, Tamura K, Miyashita Y. Reversal of interlaminar signal between sensory and memory processing in monkey temporal cortex. Science. 2011; 331:1443–1447. [PubMed: 21415353]

Tanaka K. Columns for complex visual object features in the inferotemporal cortex: clustering of cells with similar but slightly different stimulus selectivities. Cereb Cortex. 2003; 13(1):90–9. [PubMed: 12466220]

Vidu R, Rahman M, Mahmoudi M, Enachescu M, Poteca TD, Opris I. Nanostructures: A Platform for Brain Repair and Augmentation. 2014 doi: 10.3389/fnsys.2014.00091.

Wagatsuma N, Potjans TC, Diesmann M, Fukai T. Layer-Dependent Attentional Processing by Top-down Signals in a Visual Cortical Microcircuit Model. Front Comput Neurosci. 2011; 5:31. [PubMed: 21779240]

Wang M, et al. Neuronal basis of age-related working memory decline. Nature. 2011; 476:210–213. [PubMed: 21796118]

Weiler N, Wood L, Yu J, Solla SA, Shepherd GM. Top-down laminar organization of the excitatory network in motor cortex. Nat Neurosci. 2008; 11:360–366. [PubMed: 18246064]

Zhang M, Alloway KD. Intercolumnar synchronization of neuronal activity in rat barrel cortex during patterned airjet stimulation: a laminar analysis. Exp Brain Res. 2006; 169(3):311–25. [PubMed: 16284753]

Highlights

- Task-related integrated firing of prefrontal cortical minicolumns in behaving primates performing a rule-based cognitive task is reported for the first time;
- Supra-granular layers of prefrontal cortex integrate spatial information while both supra- and infra-granular layers and striatum reflect executive selection within the cognitive task;
- Glutamate recording from prefrontal cortical layer 2/3 from nonhuman primates.
- Neural prosthetic tapping into inter-laminar prefrontal microcircuits will assist patients with cortical (i.e. mini-columnar) disruption resulting from severe brain disorders.

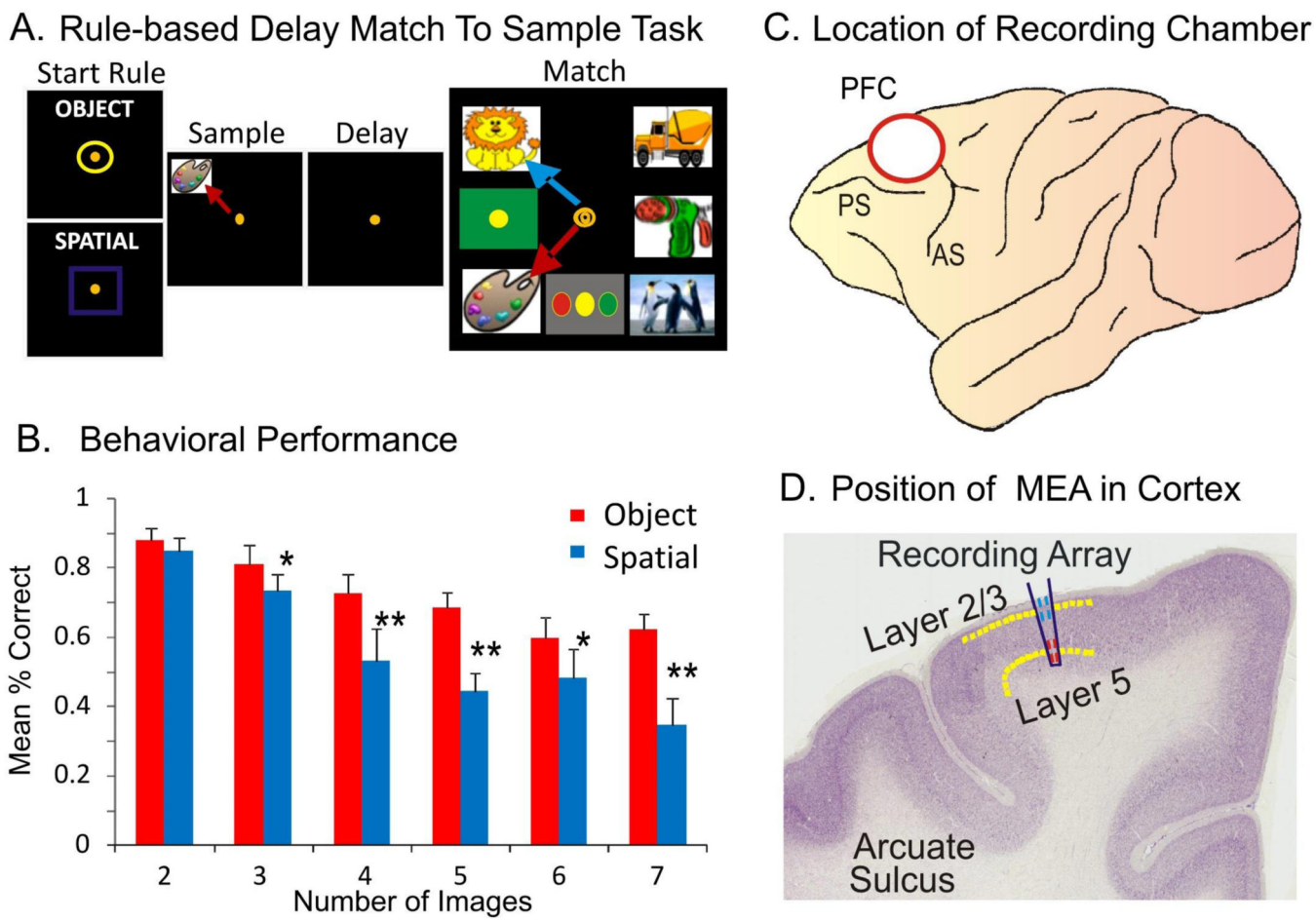

Figure 1. Simultaneous columnar-laminar recording in primate brain during cognitive tasks

A. Behavioral paradigm showing the sequence of events in the DMS task. The DMS task consisted of (1) presentation of a "Start Ring" to initiate the trial, (2) presentation of the Sample Target image, followed by (3) a variable Delay Period of 1-50 sec, prior to (4) presentation of the Match Target (i.e. Sample) image accompanied by 1-7 other Non-match (distracter) images on the same screen in which movement of the cursor into the correct image (Match response) produced juice reward via a sipper tube placed next to the animals mouth. **B.** Behavioral performance in the DMS task. Mean percent correct performance (over all animals) in Spatial (blue) and Object (red) trials. **C.** Site of the recording chamber in the prefrontal cortex (PFC) of NHP. **D.** Coronal section showing relative location of neuromorphic multielectrode array (MEA) for recording in layers 2/3 and 5.

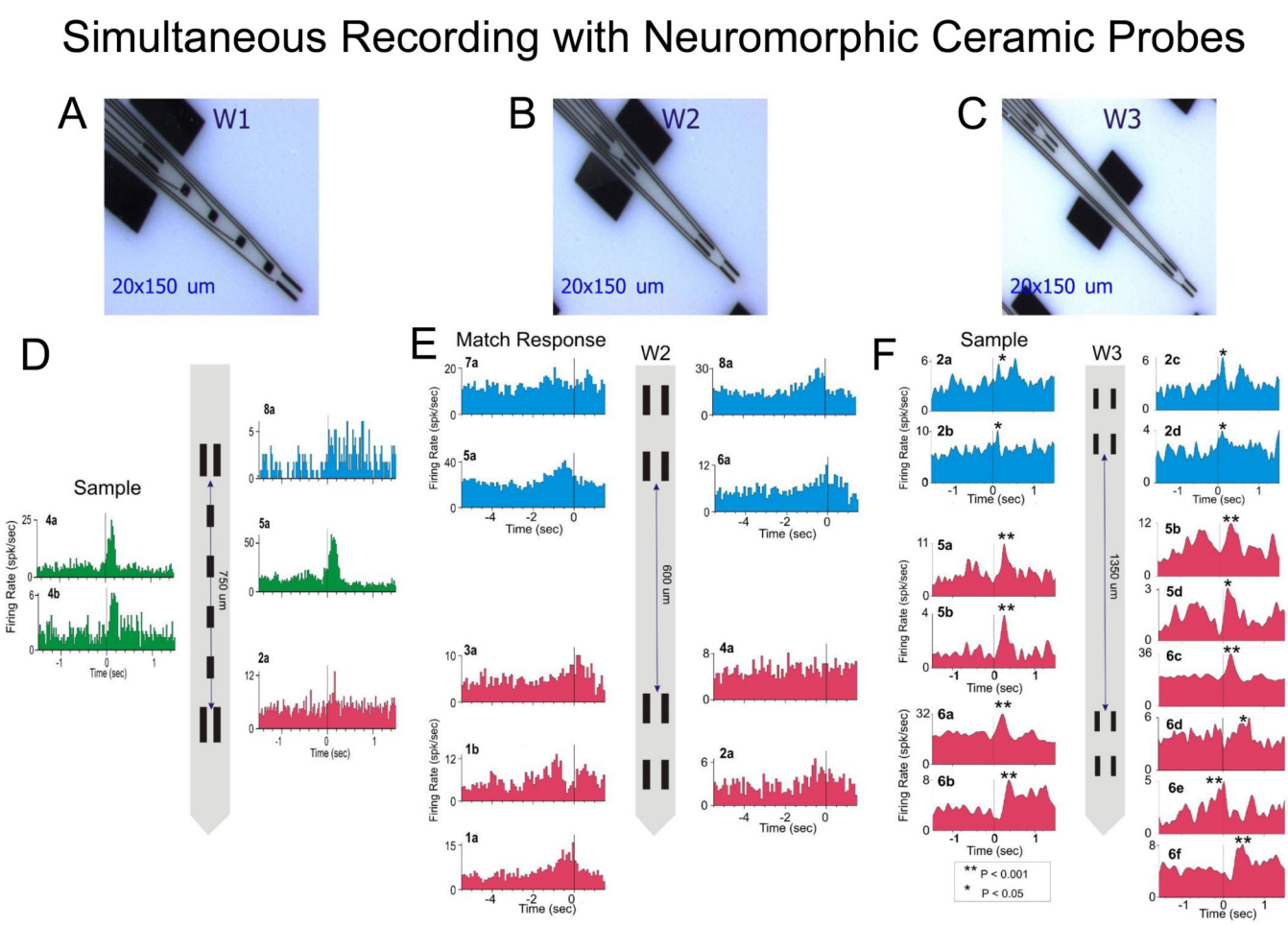

Figure 2. Example of simultaneous recordings of prefrontal neurons with neuromorphic multi-electrode arrays

A,B,C. Illustration of configuration for three different types of neuromorphic probes W1, W2, W3 used in columnar recordings. **D,E,F.** Example of simultaneous recordings in the prefrontal cortex. The code color for the neural activity in cortical layers is: layer 2/3 (blue), layer 4 (green) & layer 5 (red). Peri-event histograms (PEHs) of cell activity simultaneously recorded with neuromorphic probes during a single session. Separation distance of the recording pads is shown for each MEA diagram with cells recorded from those locations indicated by different markers.

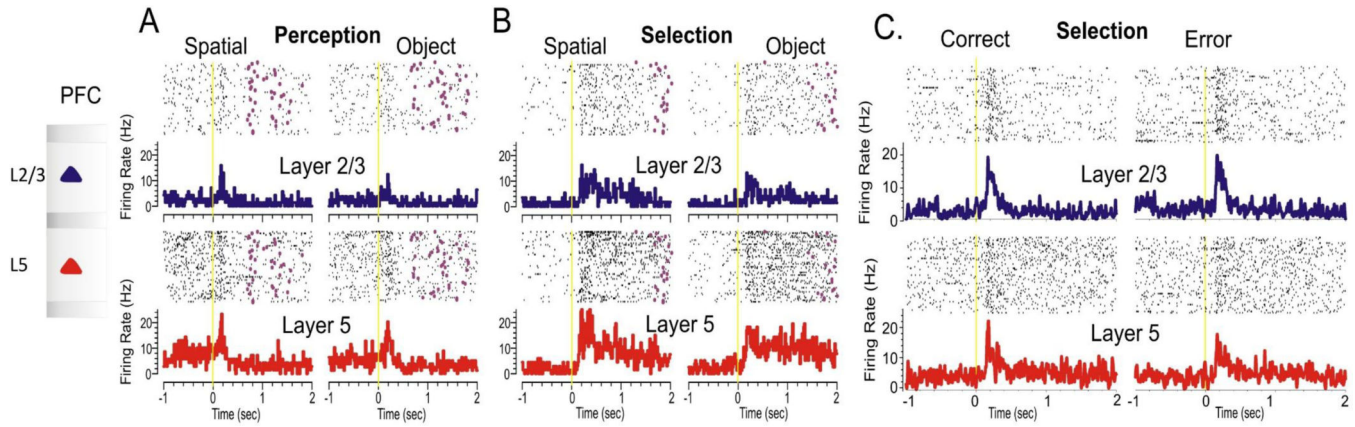

Figure 3.

Peri-event histograms and rasters showing differential firing of two neuron pairs recorded from supra (layer 2/3) and infra-granular (layer 5) layers of the prefrontal cortex. PEHs depict layers 2/3 (blue) & layer 5 (red) in the DMS task on spatial and object trials during sample (A), match (B) and correct vs. error trials (C) in the same session. Figures A & B were adapted from Opris et al, 2013 and Figure C was adapted from Opris et al. 2012a.

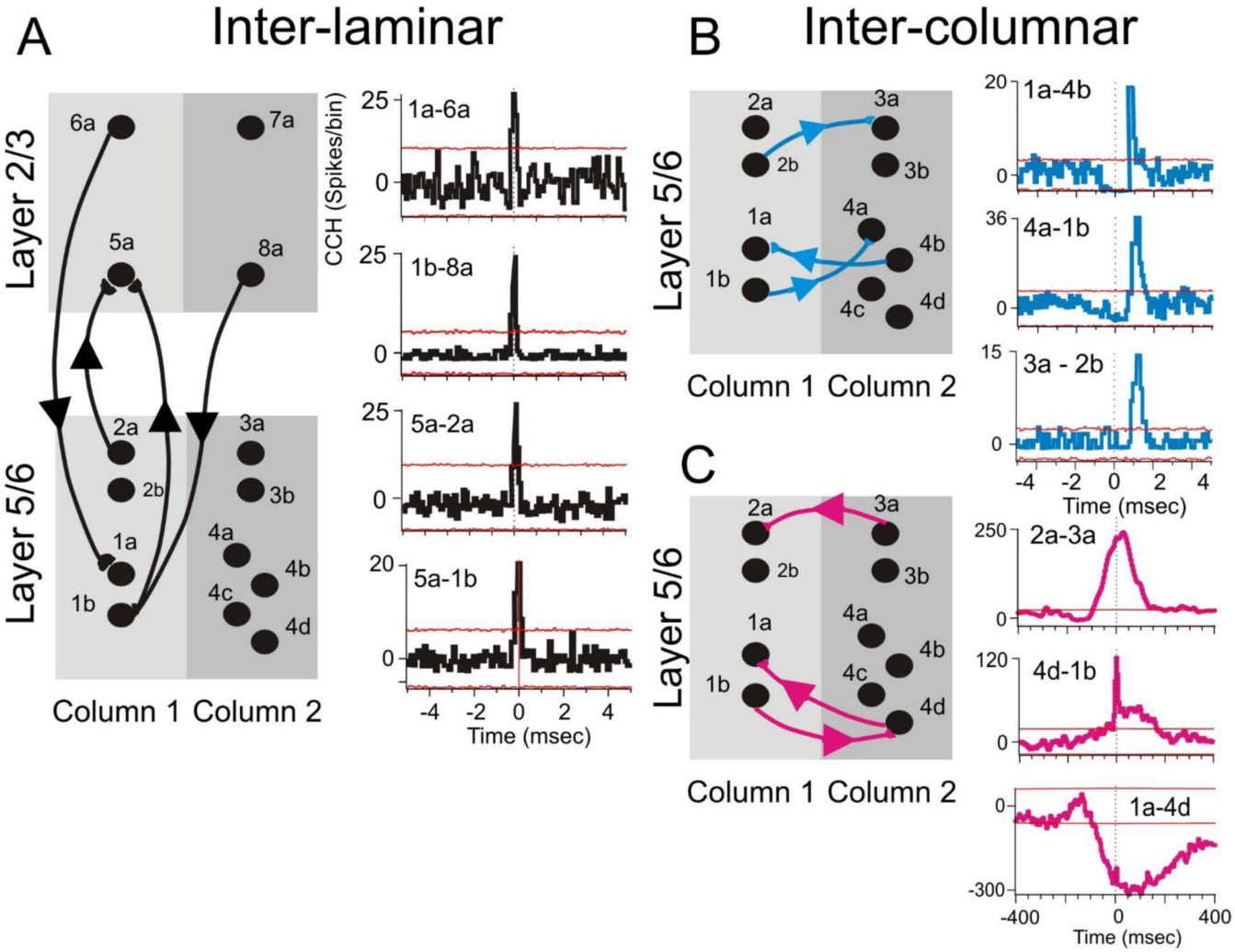

Figure 4. Complex minicolumnar firing

Cross-correlation histograms (CCHs) showed inter-laminar (**A**), inter-columnar (**B,C**) microcircuit interactions between prefrontal cells in different (or same) cortical layers and different (or same) minicolumns, respectively. To distinguish the time base of the neural interactions we used short-lag (0 to 5 ms) with binsize of 0.1 ms and long lag (0-400ms). with binsize of 5ms. The 99 % confidence intervals are depicted by red lines indicating events with significant covariant firing. Shift predictor was subtracted. This red lines indicate events with significant covariant firing.

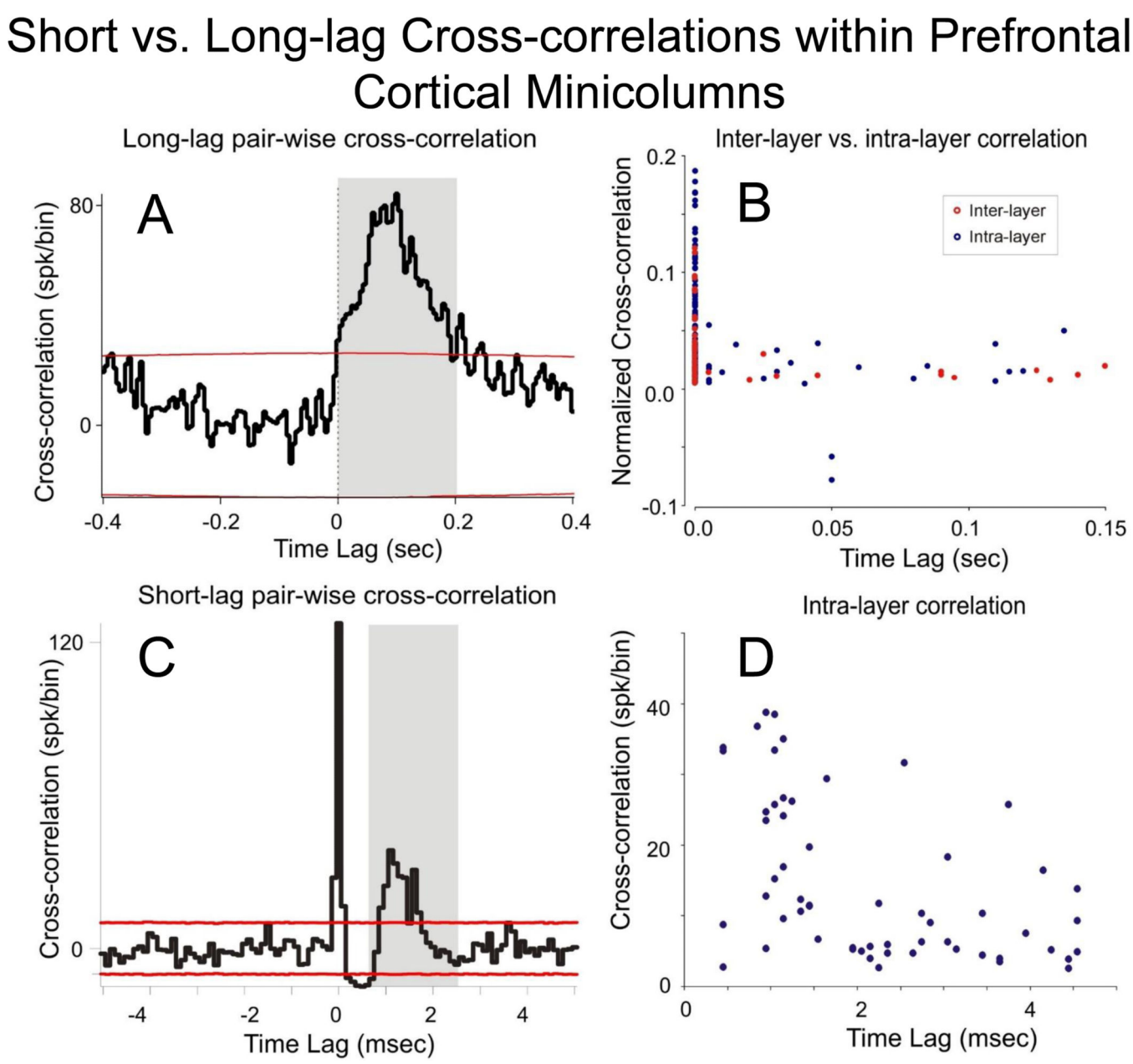

Figure 5.

A. Example of long-lag cross-correlation histogram (CCH) for an infra-granular cell pair (vertically separated by 100 μm on the MEA) with a broad peak at 50-100 msec lag (binwidth was 5 msec). **B.** Distribution of the inter-layer (red circle) vs. intra-layer (blue circle) cross-correlation peaks as a function of temporal lag. CCHs show probability of synchronized firing (ratio of extracellular spike occurrences) of layer 5 cells within ± 150.0 ms of individual spike occurrences from the layer 2/3 cell (0 ms in CCH). There were 154 intra-layer pairs and 56 of interlayer pairs. Firing synchrony calculated over entire trials between start ring onset and reward delivery. **C**. Example of short-range cross-correlation histogram (CCH) for an infra-granular cell pair (horizontally separated by 40μm on the MEA) with a central sharp peak and a broader peak having a 1-2 msec lag (binwidth was 0.1

msec). CCH provides evidence for common input on both cells in the pair and direct input from left to right cell. **D**: Distribution of the intra-layer (blue circle) cross-correlation peaks as a function of temporal lag. The 99 % confidence intervals are depicted by red lines in A & C. The mean Shift predictor was subtracted from all CCHs.

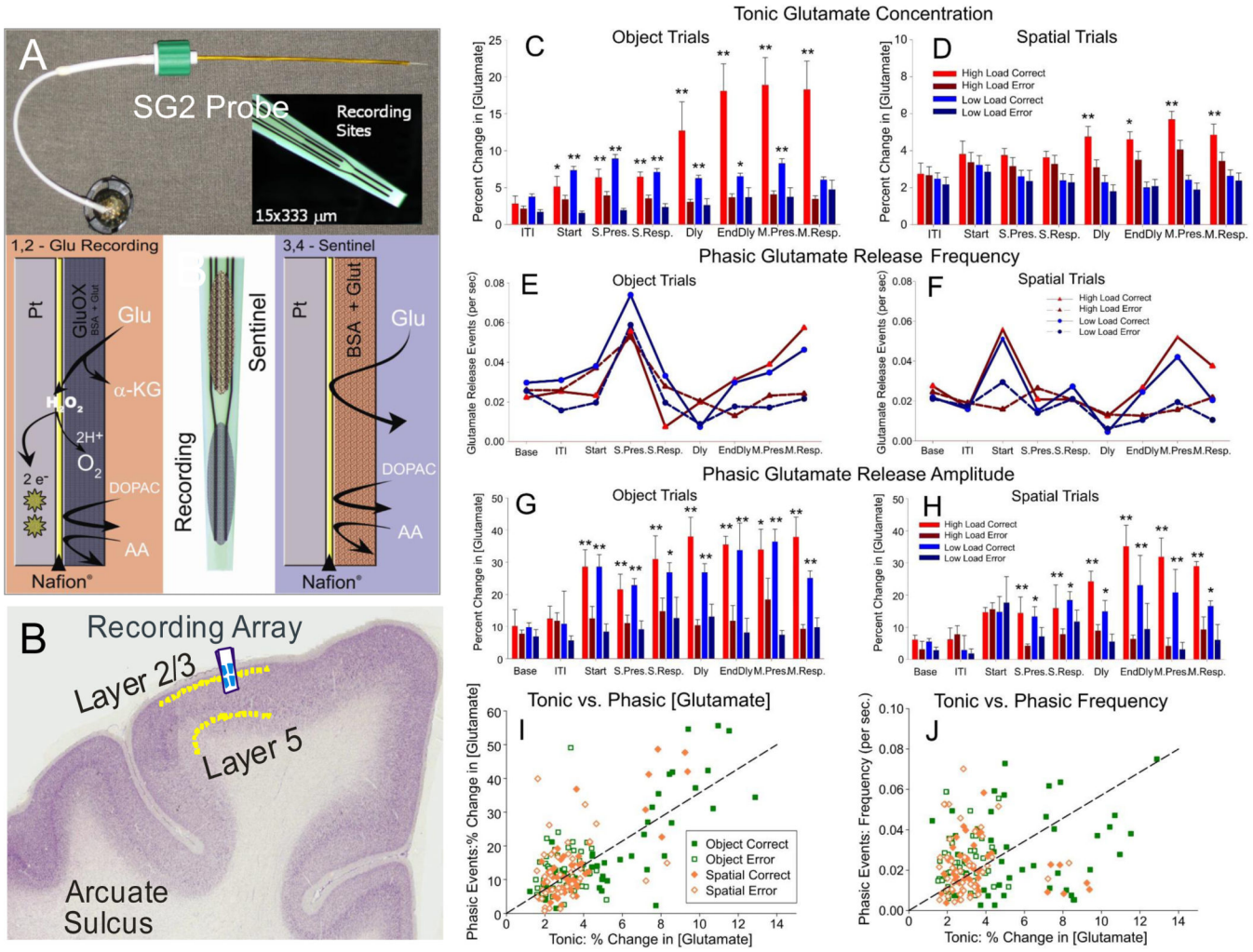

Figure 6. Glutamate Recording with Biomorphic MEAs on DMS Task

A. Spencer-Gerhardt 2 microelectrode arrays consist of four recording sites (15 x 333 µM) on a 7 cm polyimide shank that were coated with Nafion®, forming an anion exclusion layer. Dorsal recording sites (Sentinel) were coated with BSA + glutaraldehyde. The sentinel site records the current generated from any electroactive interferents that are not excluded by the Nafion® coating. Ventral recording sites were coated with Glutamate oxidase and BSA + glutaraldehyde. The GluOx coating allows the ventral pads to be sensitive to glutamate release through the enzymatic production of H_2O_2. A +0.7V potential applied to the MEA vs. Ag reference electrode oxidizes H_2O_2 resulting in a current that is directly related to the glutamate concentration. **B.** Coronal section with the MEA inserted for glutamate recording in layer 2/3 of prefrontal cortex in NHPs**. C,D.** Comparison of mean tonic glutamate concentration over 2 seconds after Match Target presentation, broken down by high/low load in correct/error trials across Spatial vs Object trials. **E,F.** Comparison of mean phasic glutamate release frequency under the same conditions across Spatial vs. Object trials. **G,H.** Comparison of mean phasic glutamate release amplitude across Spatial vs. Object trials that were successful (high load) vs. likely errors (low load) determined by assessment of neuron

firing (Figure 3). **I,J.** Scatter plots comparing % change in glutamate concentration (**I**) and frequency (**J**) of release events. **p <0.001; ANOVA analyses with post hoc tests.